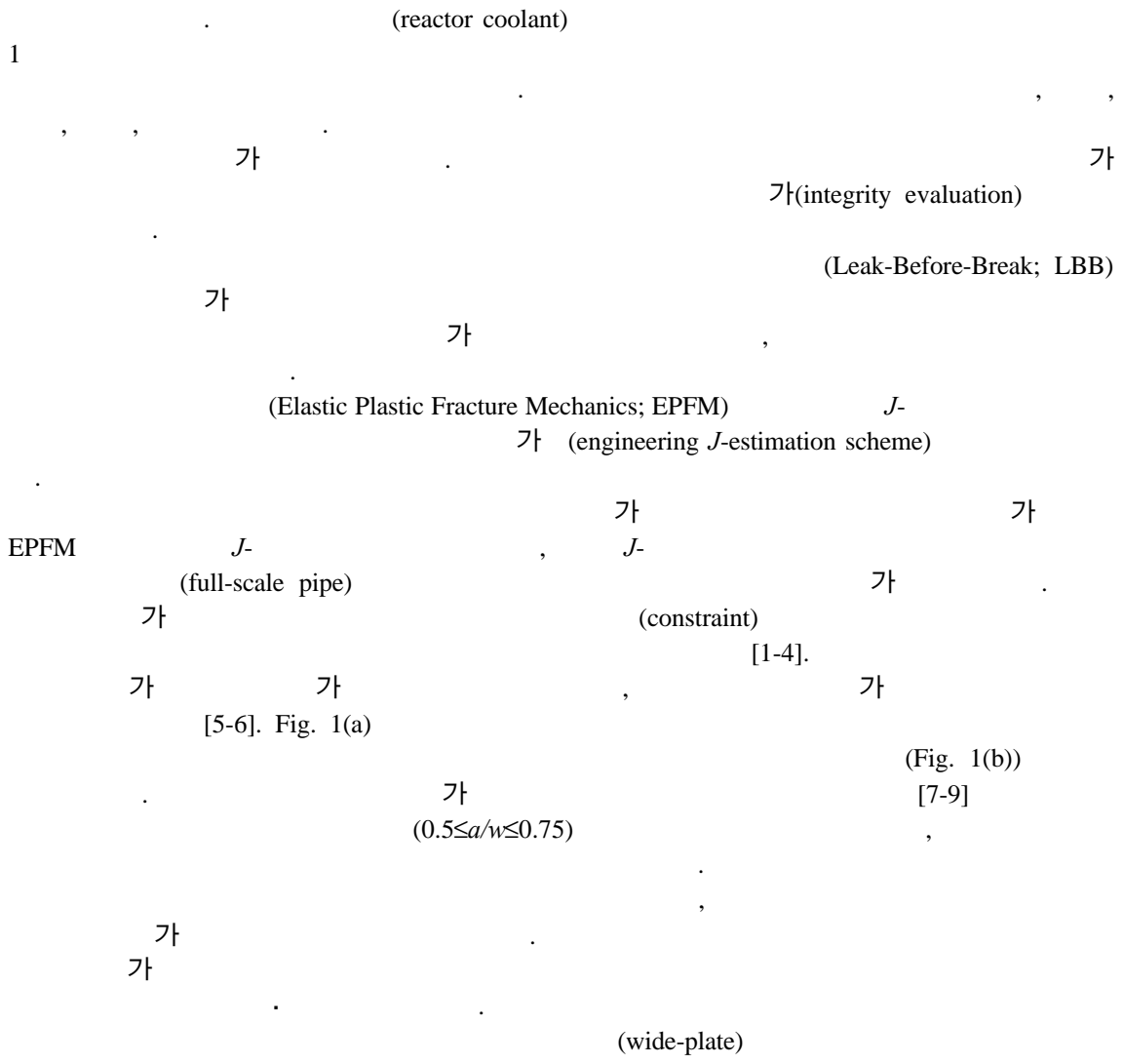
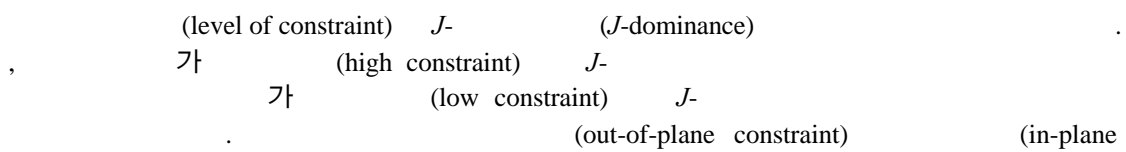


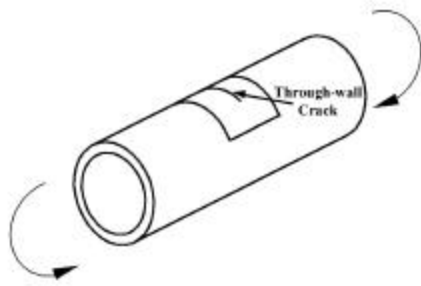
1.



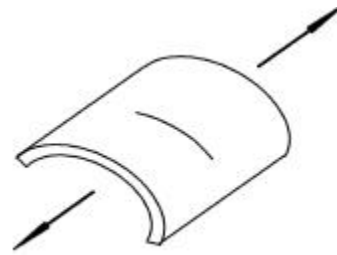
2.

2.1 (Constraint Effects)





(a) A full-scale pipe under remote bending moment



(b) A wide-plate specimen under axial tension

Fig. 1 Full-scale pipe and specimen configuration

constraint) , 가 , (width) , (remaining ligament) , 가 , (single-parameter fracture mechanics) 2 , $J-T$ [1] $J-Q$ [2,3] , 2 가 , $J-Q$ 가 .

2.2 $J-Q$

Hutchinson[10], Rice Rosengren[11] , J - Ramberg-Osgood 가 .

$$\frac{\mathbf{e}}{\mathbf{e}_0} = \frac{\mathbf{s}}{\mathbf{s}_0} + \mathbf{a} \left(\frac{\mathbf{s}}{\mathbf{s}_0} \right)^n \quad (1)$$

, \mathbf{s}_0 (reference stress) , \mathbf{e}_0 (reference strain) \mathbf{s}_0 , E , \mathbf{a} , n 가 . J - , , .

$$\mathbf{s}_{ij} = \mathbf{s}_0 \left[\frac{J}{\mathbf{a} \mathbf{e}_0 \mathbf{s}_0 I_n r} \right]^{1/n+1} \tilde{\mathbf{s}}_{ij}(\mathbf{q}, n) \quad (2)$$

$$\mathbf{e}_{ij} = \mathbf{e}_0 \mathbf{a} \left[\frac{J}{\mathbf{a} \mathbf{e}_0 \mathbf{s}_0 I_n r} \right]^{n/n+1} \tilde{\mathbf{e}}_{ij}(\mathbf{q}, n) \quad (3)$$

$$u_i = \epsilon_0 ar \left[\frac{J}{\alpha \epsilon_0 s_0 I_n r} \right]^{n/n+1} \tilde{u}_i(\mathbf{q}, n) \quad (4)$$

I_n 가 , \tilde{s}_{ij} , $\tilde{\epsilon}_{ij}$, \tilde{u}_i n \mathbf{q} ,
 (stress singularity) (2) (3) J -
 Hutchinson, Rice Rosengren (strain singularity) HRR (HRR singularity)

O' Dowd Shih[2,3] (correction factor) Q -
 가 , 3 (triaxial
 (Q -stress) J - Q Q -
 stress) (2)

$$\mathbf{s}_{ij} \approx \mathbf{s}_{ij,HRR} + Q \mathbf{s}_o \mathbf{d}_{ij} \left(\left| \mathbf{q} \right| < \frac{\mathbf{p}}{2} \right) \quad (5)$$

\mathbf{d}_{ij} Kronecker delta , (5) Q -

$$Q \equiv \frac{\mathbf{s}_{qq} - \mathbf{s}_{qq,HRR}}{\mathbf{s}_o} \quad \text{at } \mathbf{q} = 0, r = 2 \frac{J}{\mathbf{s}_o} \quad (6)$$

\mathbf{s}_{qq} , $\mathbf{s}_{qq,HRR}$ HRR
 Q - (finite strain region)
 $r/(J/s_o)=2$. Fig. 2 Q -

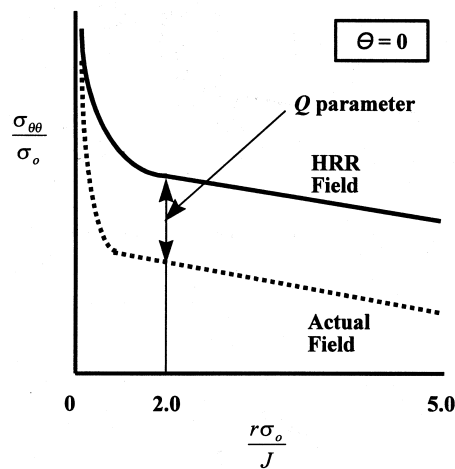


Fig. 2 A schematic illustration of the Q -stress

3.

3.1

Tension) SENB(Single Edge Notched Bending) CT(Compact Tension) 2

Fig. 3 SENB 1/2 8

ABAQUS[12] 10 (Crack Tip Opening Displacement; CTOD) 2 (large strain analysis)

가 $r/(J/s_0)$ 가 2 (small strain analysis) 20 16 가 (layer)

가 1/1000 (initial blunting radius) a/w 가 0.5 Q (6) SENB

(displacement control) Fig. 4 CT 1/2 a/w 가 0.5

Fig. 5 1/4 (flat)

plate) SENB SM45C Fig. 6

Ramberg-Osgood a n 0.025 16

3.2

Fig. 7(a) Fig. 7(b) SENB $J-Q$ 가 $J-Q$ 가

$J-Q$ 가 $J-Q$ 가 (6) Q Fig. 8 SENB $\log(J/(L \sigma))$

3 Fig. 9(a) Fig. 9(b) CT SENB 가

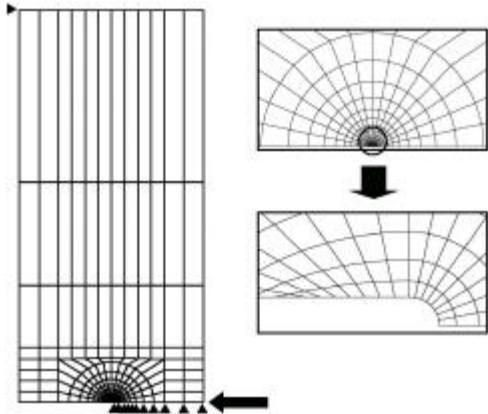


Fig. 3 Two-dimensional mesh and boundary conditions for an SENB specimen

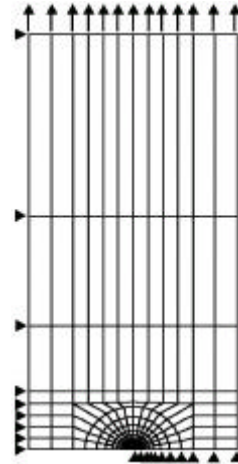


Fig. 5 Two-dimensional mesh and boundary conditions for a wide-plate specimen

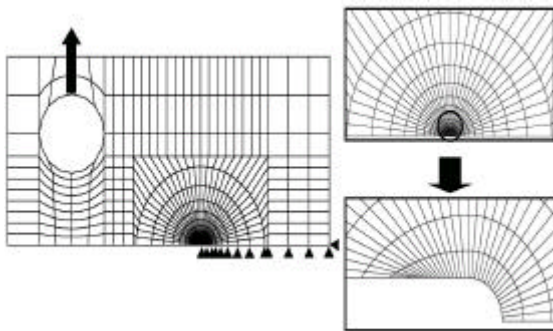


Fig. 4 Two-dimensional mesh and boundary conditions for a CT specimen

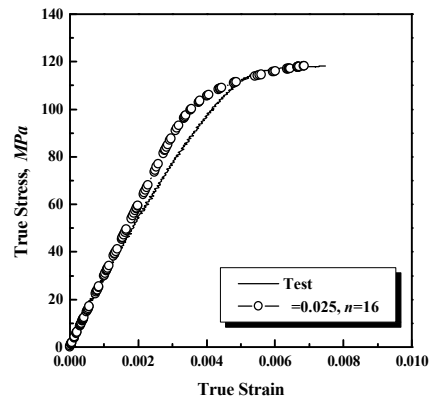
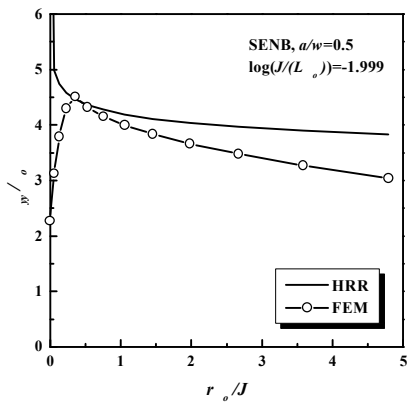


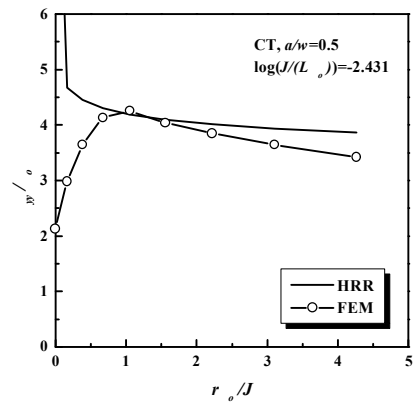
Fig. 6 True stress-strain curves for SM45C

$J-Q$ 가
 CT Q
 가 Q
 HRR
 Fig. 11(a) Fig. 11(b)
 . SENB
 가 Fig. 12 가
 가 Q 가
 $J-Q$ SENB
 SENB CT $J-Q$

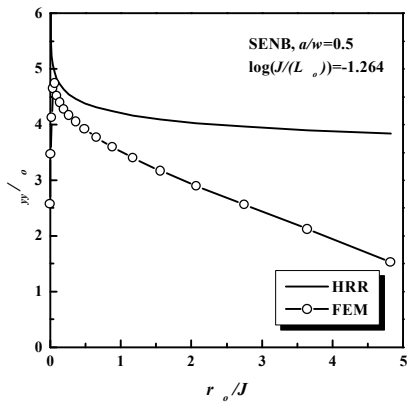
$J-Q$ 가 Fig. 10
 CT
 CT $J-Q$
 ,
 CT $J-Q$
 Q HRR
 $J-Q$ Q
 CT



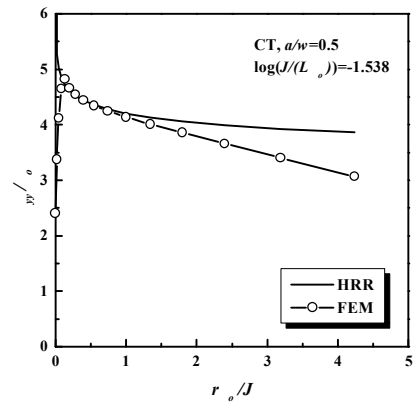
(a)



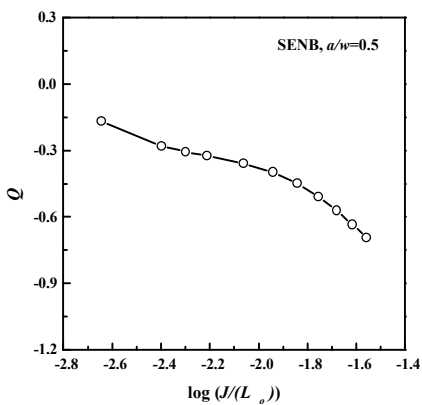
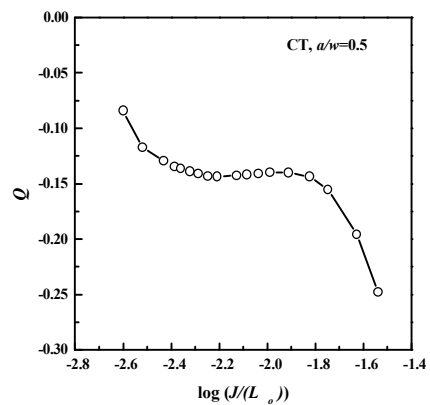
(a)



(b)



(b)

Fig. 7 J - Q stress field for an SENB specimenFig. 9 J - Q stress field for a CT specimenFig. 8 Q values for an SENB specimenFig. 10 Q values for a CT specimen

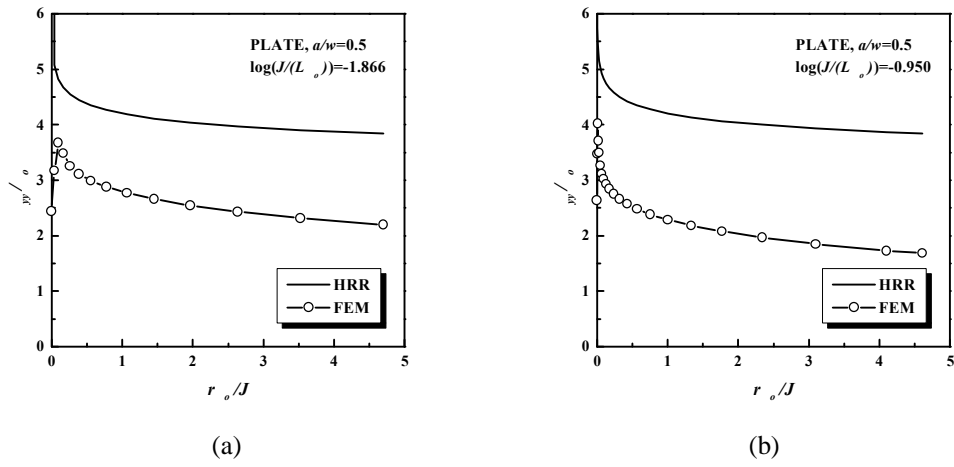


Fig. 11 J - Q stress field for a wide-plate specimen

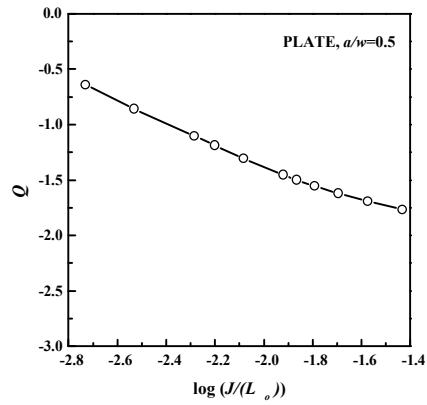


Fig. 12 Q values for a wide-plate specimen

4.

4.1

가 289mm 9mm , 가 (through-wall crack)
 2a 62mm . 200kN-m , . Fig. 13
 가 [13] , hardware-in-the-loop 가

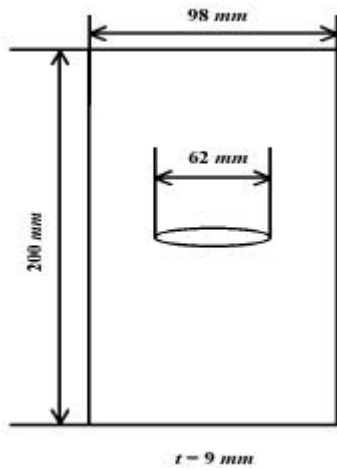


Fig. 13 The configuration of a wide-plate specimen

4.2

가 200kN-m
 15 가

Fig. 14

a 가 31mm

가

“○”

Fig. 15

가

J-
 “○”

, J- “□”

(Fig. 15 “■”)

144kN-m

J-
 SM45C

($J_{init.}$) 47,344J/m²
 (J_{IC}) 6,438J/m²

1T-CT

J-Q
 CT
 가

가

5.

가

가

(1) SENB

CT

J-Q

가

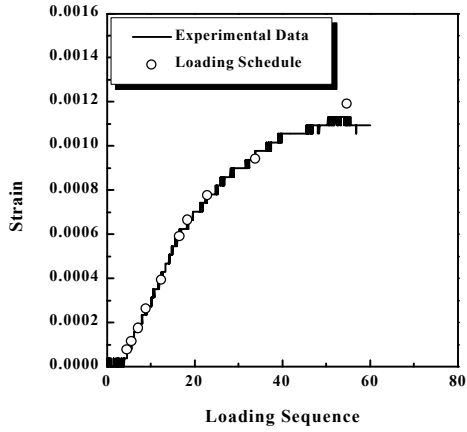


Fig. 14 Comparison of strain values between loading schedule and experimental result

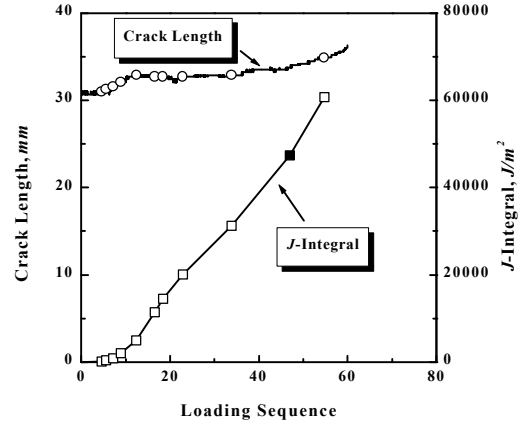


Fig. 15 Variation of crack length and J -integral measured at each loading step during the simulation

(1) SENB Q 가 가
 , CT 가 .

(2) J 가 J - Q 가
 , Q 가 가 .

(3) J - CT
 CT 가 .

가

[1] C. Betegon and J. Hancock, 1991, "Two-Parameter Characterization of Elastic-Plastic Crack-Tip Fields," *Journal of Applied Mechanics*, Vol. 58, pp. 104-110
 [2] N.P. O'Dowd and C.F. Shih, 1991, "Family of Crack Tip Fields Characterized by a Triaxiality Parameter-I, Structure of Fields," *Journal of Mechanics and Physics of Solids*, Vol. 39, No. 8, pp. 989-1015
 [3] N.P. O'Dowd and C.F. Shih, 1991, "Family of Crack Tip Fields Characterized by a Triaxiality

Parameter-II, Fracture Applications,” Journal of Mechanics and Physics of Solids, Vol. 40, No. 5, pp. 939-963

- [4] , 1997, “Constraint Pipeline Steel ,”
A, pp. 173-178
- [5] N.P. O’ Dowd and M.T. Kirk, 1993, “A Framework for Quantifying Crack Tip Constraint,” Constraint Effects in Fracture, ASTM STP 1171, pp. 2-20
- [6] J.A. Joyce, E.M. Hackett and C. Roe, 1993, “Effects of Crack Depth and Mode of Loading on the J-R Curve Behavior of a High-Strength Steel,” Constraint Effects in Fracture, ASTM STP 1171, pp. 239-263
- [7] ASTM, 1989, “Standard Test Method for J_{IC} , A Measure of Fracture Toughness,” ASTM Standard E-813-89
- [8] ASTM, 1987, “Standard Test Method for Determining J-R Curves,” ASTM Standard E-1152-87
- [9] British Standards Institution, 1991, “Method for Determination of K_{IC} , Critical CTOD and Critical J Values of Metallic Materials,” BSI 7448 – Part 1
- [10] J.W. Hutchinson, 1968, “Singular Behavior of End of a Tensile Crack Tip in a Hardening Material,” Journal of the Mechanics and Physics of Solids, Vol. 16, pp. 13-31
- [11] J.R. Rice and G.F. Rosengren, 1968, “Plane Strain Deformation near a Crack Tip in a Power-Law Hardening Material,” Journal of the Mechanics and Physics of Solids, Vol. 16, pp. 1-12
- [12] ABAQUS User’s manual, Hibbitt, Karlsson & Sorensen, Inc., 1999
- [13] , , 1999, “ 가 Hardware-in-the-Loop ,”
 , CD-Rom Title